

THE PRIMARY PROTONS AND THE ATMOSPHERIC NEUTRINO FLUXES

PAOLO LIPARI

INFN and Dipartimento di Fisica, Università di Roma "La Sapienza"

P. A. Moro 2, 00185 Roma, Italy

E-mail: paolo.lipari@roma1.infn.it

ABSTRACT

The predictions of the atmospheric ν event rates are affected by significant uncertainties, however the evidence for the ‘disappearance’ of ν_μ ’s and $\bar{\nu}_\mu$ ’s obtained by SK and other underground detectors is robust and cannot be accounted in the framework of the minimum standard model without assuming very large *ad hoc* experimental systematic effects. The existence of ‘new physics’ beyond the standard model is therefore close to be established; ν oscillations provide a very good fit to all data. The theoretical uncertainties do have an important role in the detailed interpretation of the data, and in the estimate of oscillation parameters.

1. Introduction

The experimental results of Super-Kamiokande (SK)^{1,2} and other detectors^{3,4,5,6} on atmospheric neutrinos have provided strong evidence for the existence of ν oscillations or other forms of ‘new physics’ beyond the minimum standard model. This conclusion comes from the comparison of the experimental results with theoretical predictions that have schematically the structure (for μ -like events as an example):

$$\frac{dN_\mu^{\text{th}}}{dE_\mu d\Omega_\mu} = \sum_{\alpha=e,\mu} [\phi_0 \otimes Y_{p,n \rightarrow \nu_\alpha} \otimes P(\nu_\alpha \rightarrow \nu_\mu)] \otimes \sigma_\nu \otimes A_{\text{det}} \quad (1)$$

where N_μ^{th} is the predicted μ event rate, E_μ and Ω_μ are the muon energy and direction, and the different ingredients of the prediction are: (i) ϕ_0 the primary cosmic ray (c.r.) flux; (ii) $Y_{p(n) \rightarrow \nu_\alpha}$ the ν yield, that is the number of neutrinos of flavor α produced in p (n) induced c.r. showers; (iii) σ_ν the neutrino cross sections; (iv) $P(\nu_\alpha \rightarrow \nu_\beta)$ the oscillation probability; and (v) A_{det} the detector acceptance. We have dropped all dependences on flavor, energy and zenith angle of the different elements and the symbol \otimes indicates the need for appropriate convolutions that can be done accurately only with Montecarlo methods.

The fundamental result obtained with the measurements of atmospheric ν ’s is that the data *cannot* be described in the minimum standard model, (in the absence of oscillations). In particular the ν_μ survival probability $P(\nu_\mu \rightarrow \nu_\mu)$ must be smaller than unity in a large region of energy and ν pathlength. In short: muon neutrinos disappear.

It is possible to go beyond this fundamental but qualitative statement. With

the inclusion of ν -oscillations one can obtain a good description of the data and extract quantitative information on the ν masses and mixing.^a Two flavors $\nu_\mu \leftrightarrow \nu_\tau$ oscillations with maximal or very large mixing are a viable explanation for the data. The determination of the ν oscillation parameters is of course of fundamental importance, and has also a crucial role to determine the best strategy for future experimental studies.

In this work we will analyse the first three elements of the predictions: the primary flux, the modeling of hadronic showers and the ν cross sections (without considering at all the important questions of detector acceptance and background estimates), and discuss what are the effects of the existing uncertainties. We will argue that the fundamental result that the minimum standard model fails to describe the atmospheric ν data is robust, and that the evidence for the disappearance of ν_μ 's cannot be “re-absorbed” taking into account theoretical uncertainties. On the other hand these uncertainties can play a significant role in the interpretation of the data and in the determination of the oscillation parameters.

In this work we will refer to some published calculations of the atmospheric ν fluxes. Two detailed Monte Carlo (MC) calculations of the fluxes performed by the Bartol group⁹ and by Honda, Kajita, Kasahara and Midorikawa (HKKM)¹⁰ have been used to compute predictions for the interpretation of the existing data. Other calculations have been performed analytically by Bugaev and Naumov¹¹ or again with MC methods by Lee and Koh¹². A new detailed calculation using the FLUKA code¹³ for the modeling of hadronic interaction is close to completion¹⁴.

This discussion is organized as follows. In the next section we will briefly discuss the evidence for new physics in the atmospheric ν data; in section 3 we will describe some predictions for the atmospheric ν fluxes; in section 4, 5 and 6 we will consider the three main elements in the prediction: the primary cosmic ray flux, the development of hadronic showers; and the ν cross sections; in section 7 we will consider the constraint coming from atmospheric muon measurements; in section 8 we discuss the question of the absolute normalization of the ν flux; in section 9 we will discuss some possible effects of the uncertainties in the predictions for the determination of the oscillation parameters.

2. Evidence for the disappearance of ν_μ 's

The evidence for the disappearance of muon (anti)-neutrinos comes from the observation of three experimental effects, listed here in order of ‘robustness’: (i) the detection of an up-down asymmetry for the μ -like events, (ii) the detection of a

^a Other mechanisms, different from oscillations, such as ν decay, FCNC, or violations of the equivalence principle, have been proposed as explanations of the disappearance of the muon neutrinos. These alternative or ‘exotic’ models provide (at least until now) significantly less satisfactory description of the data. See^{7,8} for more discussion.

small μ/e ratio, (iii) the detection of a distortion of the zenith angle distribution and a suppression of the ν induced upward going muon flux.

Some comments about the first two effects can be made already before entering in a detailed discussion of the prediction because two properties of the ν fluxes: an approximate up-down symmetry, and a strongly constrained ν_μ/ν_e ratio, are to a large extent independent from the details of the calculation and provide ‘self calibration’ methods.

(i) The ν fluxes are predicted in the no-oscillation hypothesis to be approximately up/down symmetric:

$$\phi_{\nu_\alpha}(E_\nu, \theta) \simeq \phi_{\nu_\alpha}(E_\nu, \pi - \theta) \quad (2)$$

This follows as a simple and *purely geometrical* theorem from two assumptions: (a) the primary c.r. flux is isotropic, (b) the Earth is spherically symmetric. The geomagnetic field, as will be discussed in some detail in section 4.2, is the most important source of up-down asymmetry. The theory predicts unambiguously that the effects of the geomagnetic field are small, decreasing with E_ν and for Kamioka produce an excess of *up-going* particles. This predictions have received an important quantitative experimental confirmation with the measurement of the east-west effect in SK¹⁵, that is also produced by the geomagnetic field, and is largely independent from oscillations¹⁶. For the sub-GeV and multi-GeV muon samples in SK the up/down asymmetry $A = (U - D)/(U + D)$ (where U (D) is the number of up (down) going events with $\cos\theta_\mu \leq -0.2$ ($\cos\theta_\mu \geq -0.2$) takes the values:

$$A_{sub} = -0.150 \pm 0.028 \pm 0.01 \quad A_{mul} = -0.311 \pm 0.043 \pm 0.01 \quad (3)$$

these are deviations of 5.4 and 7.2 standard deviations from no asymmetry.

(ii) The ν_μ and ν_e fluxes are strictly related to each other because they are produced in the chain decay of the same charged mesons (as in $\pi^+ \rightarrow \nu_\mu \mu^+ \rightarrow \nu_\mu (\bar{\nu}_\mu \nu_e e^+)$):

$$\phi_{\nu_\mu}(E, \theta) = r_\nu(E_\nu, \theta) \times \phi_{\nu_e}(E, \theta) \quad (4)$$

the factor $r_{\nu(\bar{\nu})}(E_\nu, \theta)$ vary slowly with energy and angle is quite insensitive to the details of the calculation. At low energy when essentially all parent muons decay before reaching the ground one has $r_{\nu(\bar{\nu})} \simeq 2$. This is in agreement with a naive ν ‘counting’ argument. This simple argument is approximately valid because after chain decay the three neutrinos produced in the decay of a pion have similar average energy (for ultrarelativistic $\pi^+ \rightarrow \nu_\mu (\bar{\nu}_\mu \nu_e e^+)$ decay one has: $\langle E_\nu/E_\pi \rangle = 0.213, 0.265$ and 0.257 for the ν_μ , $\bar{\nu}_\mu$ and ν_e channels). With increasing energy, because of the Lorentz time dilatation, the muons begin to reach the ground before decay and $r_{\nu(\bar{\nu})}$ increases, with a stronger (weaker) effect for vertical (horizontal) directions because of the different distance between the primary interaction point and the ground. These energy and zenith angle dependence of r (see fig. 1) are controlled essentially by

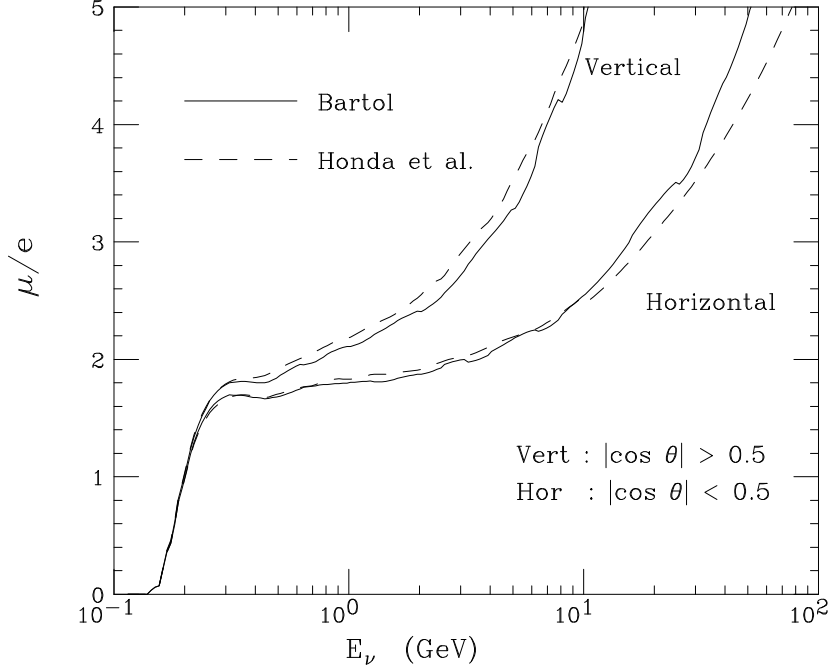


Fig. 1. μ/e ratio of ν -interacting ν 's calculated in the no-oscillation hypothesis using the Bartol⁹ and HKKM¹⁰ fluxes.

geometry and reliably calculable. In SK the the double ratio $R = (\mu/e)_{data}/(\mu/e)_{MC}$ for the sub-GeV and multi-GeV samples are measured as:

$$R_{sub} = 0.668^{+0.026}_{-0.023} \pm 0.007 \pm 0.052 \quad R_{mul} = 0.663^{+0.044}_{-0.041} \pm 0.013 \pm 0.078 \quad (5)$$

where the errors are statistical, systematic and theoretical (as estimated by SK). Combining in quadrature all errors the significance of the deviations of the double ratios from unity are 5.7 and 3.7 standard deviations. The uncertainty in the denominator of the double ratios has several sources: the ratio π^+/π^- (that determines ratio $\nu_e/\bar{\nu}_e$ important because of the different cross sections of ν 's and $\bar{\nu}$'s), the contribution of kaons^b, the shape of the primary spectrum, and the momentum distribution of the produced mesons. These uncertainties have estimated^{1,19,20} as of order 5% for a fixed value of E_ν . Since experimentally the (μ/e) implies an integration over a finite interval of energy and the convolution of the ν spectra with detection efficiency curves that are flavor dependent, an important source of uncertainty comes from the knowledge of the shape of the energy spectrum, and the energy dependence of the ν cross section. For this reason the uncertainty on $(\mu/e)_{MC}$ is larger than 5% and was estimated by

^bIn the chain decay $K^+ \rightarrow \nu_\mu \mu^+ \rightarrow \nu_\mu (\bar{\nu}_\mu \nu_e e^-)$ the average energy of the three neutrinos is $\langle E_\nu/E_K \rangle = 0.477, 0.159$ and 0.205 , therefore for neutrinos from K decay the naive ν 'counting' argument is not valid. This is compensated by the fact that charged and neutral kaons are also a source of electron neutrinos via the decays $K \rightarrow \pi e \nu_e$.

SK as 8% and 12% for the sub-GeV and multi-GeV sample. The estimate of the value and uncertainty of the denominator in the double ratios is very important for the interpretation of the data. In any case even with a very conservative estimate of ‘theoretical errors’ it does not appear possible to explain the detected low values of R obtained without appealing to *experimental* errors in flavor identification.

(iii) For the interpretation of the upward-going muon data, the methods of comparing up and down hemispheres, or the ν_μ and ν_e fluxes are not available, therefore the uncertainties in the predictions are more important. The angular distribution of the muons, and the ratio between a high energy and a low energy part of the signal (or example stopping and through-going muons), are less sensitive to the model (see ¹⁷ for a critical discussion), and provide important tools for the interpretation of the data¹⁸. Upward going muons are the best way to study the ν_μ fluxes at high E_ν , and this is important to study experimentally the energy dependence of the ν flavor transitions⁸.

3. Neutrino Fluxes calculations

In this section we will briefly present some results about the properties of the calculated neutrino fluxes. For the sake of clarity, we will discuss the ν event rate that (for example for e -like events) can be calculated as:

$$\frac{d^2 N_e}{dE_\nu d\cos\theta_\nu} = N_A [\phi_{\nu_e}(E_\nu, \cos\theta_\nu) \sigma_{\nu_e}^{CC}(E_\nu) + \phi_{\bar{\nu}_e}(E_\nu, \cos\theta_\nu) \sigma_{\bar{\nu}_e}^{CC}(E_\nu)] \quad (6)$$

as the product of the flux times the neutrino cross sections. For σ_ν we will use in this work the estimates of ²¹ including nuclear effects.

In fig. 2 we show the energy distributions of up-going and down-going interacting neutrinos at Kamioka as calculated for minimum solar activity, by the Bartol⁹ and HKKM¹⁰ groups. The ν direction was integrated over the angular regions: $\cos\theta_\nu \in [-1, 0]$ for ‘Up’ events, or $\cos\theta_\nu \in [0, 1]$ for ‘Down’ events. Plotting $E_\nu dN/dE_\nu = dN/d\ln E_\nu$ with a logarithmic energy scale, the area below the curve is proportional to the total rate. Some remarks about fig. 2:

(i) The two calculations, especially for $E_\nu \gtrsim 1$ GeV, are quite similar to each other both in absolute normalization and in the shape of energy distribution. This similarity, as it will be discussed later, is to some extent the result of a cancellation of a higher (lower) primary cosmic ray flux and a lower (higher) ν yield per primary particle for the HKKM (Bartol) calculation.

(ii) Both calculations predict that the up-going and down-going ν fluxes become equal for $E_\nu \gtrsim 1$ GeV. At low energy (and in the absence of oscillations) the calculations predict a higher up-going flux. This is the result of the geomagnetic effects and has *opposite* sign with respect to the effect of oscillations. It should be noticed that the Bartol calculation predicts a stronger no-oscillation up-down asymmetry for

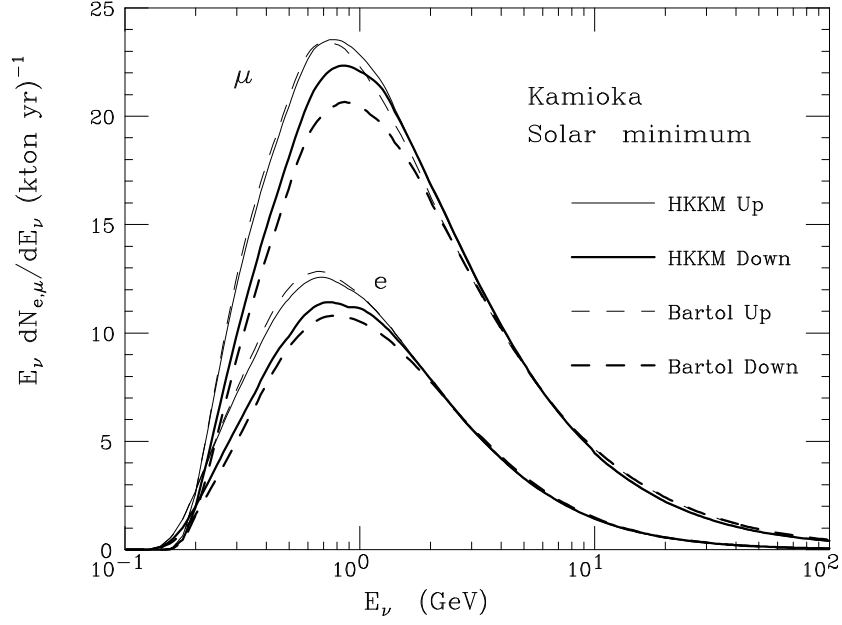


Fig. 2. Energy distributions of up-going ($\cos \theta_\nu < 0$) and down-going ($\cos \theta_\nu > 0$) cc-interacting ($\nu_e + \bar{\nu}_e$)'s and ($\nu_\mu + \bar{\nu}_\mu$)'s at Kamioka. The calculations are for solar minimum and with the Bartol⁹ and HKKM¹⁰ ν fluxes.

neutrinos with $E_\nu \lesssim 1$ GeV.

The calculated ν event rates depend on the detector position and the epoch of solar activity. This is illustrated in table 1 and 2, that give the charged current event rates (with no detector efficiency or requirement for containment included) for two detector positions (the Kamioka and Soudan mines) and different levels of solar activity. For the Kamioka site, we also compare the two MC calculations of Bartol and HKKM. The quantities (U_L , U_H , D_L and D_H) refer to an integration in the ν zenith angle in the regions: $\cos \theta_\nu \in [-1, 0]$ for ‘Up’ events, or $\cos \theta_\nu \in [0, 1]$ for ‘Down’ events, and an integration in energy $E_\nu \leq 1$ GeV for ‘Low’ energy and $E_\nu \geq 1$ GeV for ‘High’ energy. The asymmetry is calculated as $A = (U - D)/(U + D)$. Some remarks can be useful:

- (i) For sufficiently large E_ν ($E_\nu \gtrsim 1$ GeV) the calculated event rate is: (a) independent from energy, (b) independent from the detector position, and (c) up/down symmetric. Conversely at low energy there is a significant dependence on detector location and solar epoch, and there are significant deviations from up/down symmetry even in the absence of oscillations.
- (ii) At the epoch of solar minimum, that to a good approximation applies to the data taking period of SK (see fig. 7), without considering the effect of detector efficiency, the rates of e -like events with $E_\nu \leq 1$ GeV ($E_\nu \geq 1$ GeV) in Soudan and SK are predicted by the Bartol calculation to be in the ratio: Soudan/Kamioka $\simeq 1.72$ (1.17).

Table 1. Event rates (kton yr)^{−1} and Up/Down asymmetry for e like event.

Site	Flux	⊙	U_L^e	D_L^e	A_L^e	U_H^e	D_H^e	A_H^e
Kamioka	HKKM	min	15.8	13.5	0.077	14.5	14.4	0.002
Kamioka	HKKM	mid	15.1	13.1	0.070	14.2	14.2	0.001
Kamioka	HKKM	max	14.3	12.7	0.060	13.9	13.9	0.000
Kamioka	Bartol	min	16.2	12.5	0.129	14.6	14.2	0.013
Kamioka	Bartol	max	14.3	12.2	0.077	14.3	14.1	0.006
Soudan	Bartol	min	20.7	28.4	−0.158	16.3	17.6	−0.039
Soudan	Bartol	max	17.5	21.9	−0.112	15.8	16.8	−0.031

Table 2. Event rates (kton yr)^{−1} and Up/Down asymmetry for μ like event.

Site	Flux	⊙	U_L^μ	D_L^μ	A_L^μ	U_H^μ	D_H^μ	A_H^μ
Kamioka	HKKM	max	27.5	24.4	0.059	34.3	34.2	0.001
Kamioka	HKKM	mid	26.5	23.8	0.053	33.8	33.8	0.000
Kamioka	HKKM	max	25.2	23.0	0.046	33.1	33.2	0.000
Kamioka	Bartol	min	27.8	22.3	0.109	33.9	33.4	0.008
Kamioka	Bartol	min	25.1	21.9	0.067	33.5	33.3	0.004
Soudan	Bartol	min	34.1	44.8	−0.136	36.4	38.4	−0.026
Soudan	Bartol	max	29.8	36.5	−0.100	35.8	37.3	−0.021

The experimental results suggests a lower ratio (see section 7 for more discussion).

(iii) All event rates should be reduced during the future period of solar maximum, with a significantly larger reduction for Soudan because of the lower geomagnetic cutoff. As an illustration, the ratio (\odot max)/(\odot min) for sub-GeV e -like events is predicted by the Bartol calculation to be ~ 0.80 for Soudan and ~ 0.93 for Kamioka. These time variations should be measurable and offer a handle for a check of the predictions.

(iv) At low energy the geomagnetic effect result in a significant up-down asymmetry even in the absence of oscillations. It is remarkable that this asymmetry has opposite signs at Soudan (with an excess of down-going ν 's) and Kamioka (excess of up-going ν 's). This effect is also illustrated in fig. 3. The difference between Soudan and Kamioka can be easily understood qualitatively taking into account the fact that the magnetic latitudes of Kamioka and Soudan are $\lambda_M \simeq 27^\circ$ and 56° , and the different geomagnetic cutoffs for the two locations (see section 4.2).

3.1. The response function

Fig. 4 is taken from Gaisser²⁰ and shows the energy distribution of the primary particles that (would) contribute to the to the μ -like sub-GeV signal in Super-Kamiokande. The solid (dotted) curves are for solar minimum (maximum). The pair of curves indicated as B (C) are the response curves for up-going (down-going)

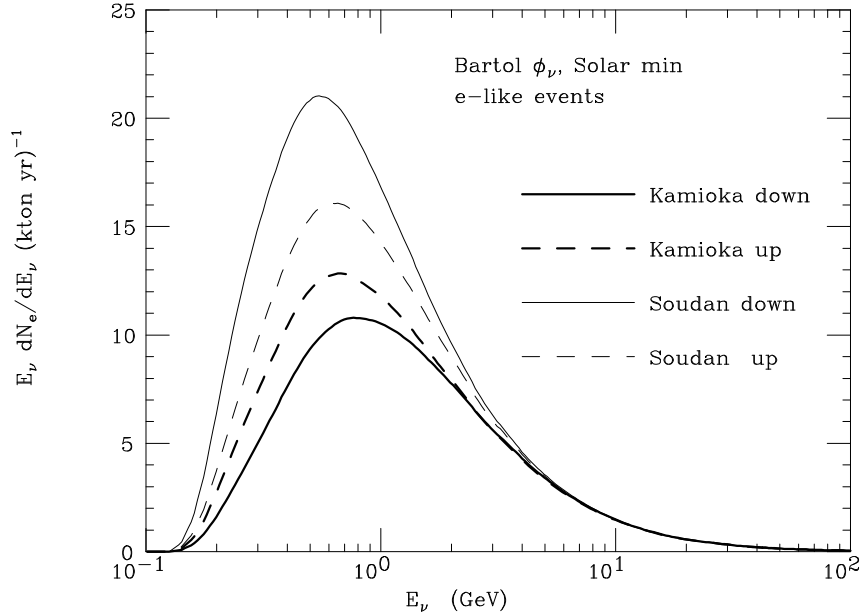


Fig. 3. Energy distributions of up-going ($\cos \theta_\nu < 0$) and down-going ($\cos \theta_\nu > 0$) interacting ν_e 's and $\bar{\nu}_e$'s at Kamioka and Soudan. The calculations are based on the solar minimum Bartol ν fluxes.

neutrinos at Kamioka. One can notice how the lower flux of the down-going hemisphere originates from the higher geomagnetic cutoffs relevant for the low magnetic latitude site of Kamioka. Curve A is calculated assuming zero cutoff and is a reasonable approximation for the down-going ν flux of the high magnetic latitude of Soudan where geomagnetic cutoffs are small. The primary energies that are important for the atmospheric ν signal are in a broad range $E_0 \sim 3\text{--}100$ GeV. It is also important to notice that experiments made in different locations will be sensitive to somewhat different ranges of primary energy, and that in particular the event rates at Soudan receive a large contribution, from particles with $E_0 \simeq 10$ GeV, and the prediction is very sensitive to the flux and interaction properties of low energy primaries.

4. The primary cosmic ray flux

The primary cosmic ray flux has been a major source of uncertainty (see²⁰ for a detailed discussion) because of the discrepant results obtained by two groups: Webber²² and LEAP²³), differing by $\sim 50\%$ (see fig. 5). In more recent time there have been four new measurements of the p flux: IMAX²⁴, CAPRICE²⁵, BESS²⁶ and MASS²⁷) of the proton flux (some including also measurement of higher mass primaries). All four these new measurements (shown in fig. 5) are, at least qualitatively, in agreement between each other and confirm the lower normalization of the LEAP²³ experiment.

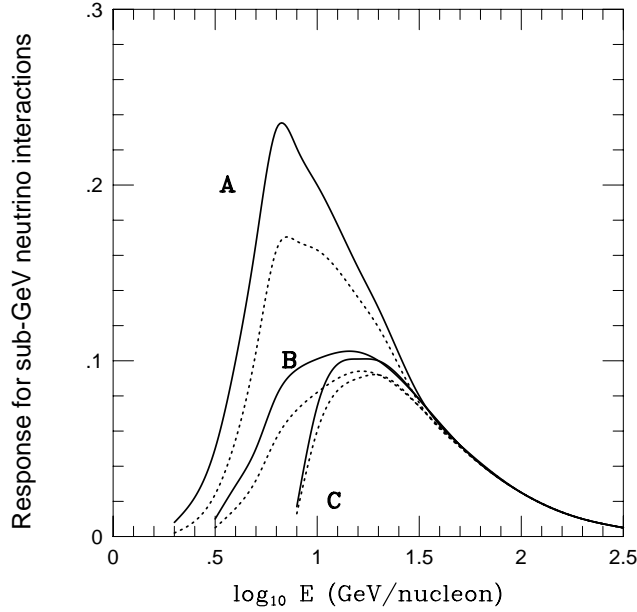


Fig. 4. From Gaisser²⁰. Energy distribution of primary particles that produce the sub-GeV μ -like event rate in Super-Kamiokande (see text).

The conclusion is that, if one is ready to discard the early measurement of Webber²², the primary flux is much better determined, with an uncertainty in the relevant region of better than 10%.

It is important to compare the new experimental results on the p flux with the representations chosen for the calculations of the ν fluxes. This comparison is shown in fig. 5 and in more detail in fig. 6. where the data and the different descriptions of the p flux are shown as a ratio with respect to the proton flux used in the HKKM¹⁰ calculation for minimum solar activity. The three thin solid lines describe the p flux assumed for by HKKM for minimum, medium and maximum solar activity (upper line with constant value of unity, middle line and lower line). The thick line is the description of the p flux at solar minimum used in the Bartol calculation. Only two sets of data points are shown, those obtained by the Caprice²⁵ and MASS2²⁷ experiments. These data were obtained in 1997 and 1991 approximately at the epoch of minimum (maximum) solar activity. Some remarks:

- (i) The measurements are consistent with each other for $E_p \gtrsim 10$ GeV. Below this energy the difference in the measured flux, agrees with the expectations for the solar modulation.
- (ii) For $E_p \gtrsim 10$ GeV, the descriptions of the p flux used in the calculations of the ν fluxes are in poor agreement with the data. The discrepancy is *not* a constant factor. As an illustration in fig. 6 we have included a dot-dashed line: $(E_p/7 \text{ GeV})^{-0.22}$, that corresponds very roughly to the ratio data/model for the solar minimum p flux of

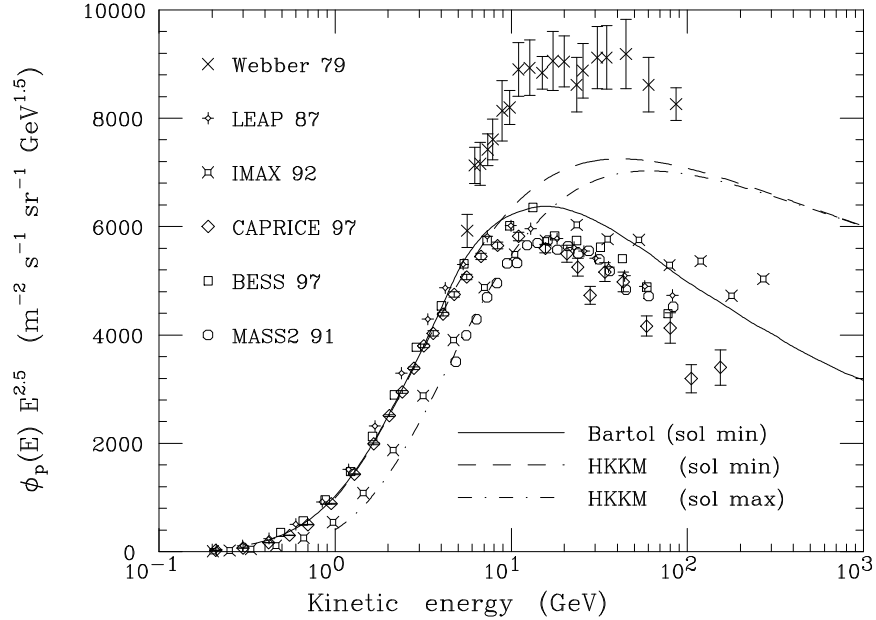


Fig. 5. Measurements of the c.r. proton flux (points) and the representations used as input in the Bartol and HKKM calculations (lines).

HKKM, and a dashed line $(E_k/9.5 \text{ GeV})^{-0.144}$), that corresponds roughly to the ratio Bartol/HKKM at solar minimum.

4.1. Time dependence

The time variability of the primary cosmic ray flux is caused by the time varying structure of the heliosphere, that is on the electro-magnetic fields that fills the interplanetary space and are the result of the interaction of the solar wind (an out-flow of plasma from the sun) with the interplanetary medium. The topics of the structure of the heliosphere, and the phenomenon of the modulation of cosmic rays (the two topics are of course strictly related since the c.r. modulations are an important tool to study the characteristics and dynamics of the heliosphere) are very complex (see ²⁸ for a review and references) and will not be discussed here. It can only be said that because of the presence of the solar wind plasma and the e.m. fields associated with it, for cosmic rays the heliosphere is a medium that goes from semi-transparent (for rigidity $R \sim 5 \text{ GeV}$) to totally opaque (for kinetic energy of few hundred MeV/nucleon). The transparency of the medium depends on the intensity of the solar wind, that is correlated with the intensity of the solar magnetic activity, and varies with an 11 years period (22 years considering also the polarity of the magnetic field). This magnetic activity can be monitored for example with measurements of the number of sunspots. The correlation between the cosmic ray

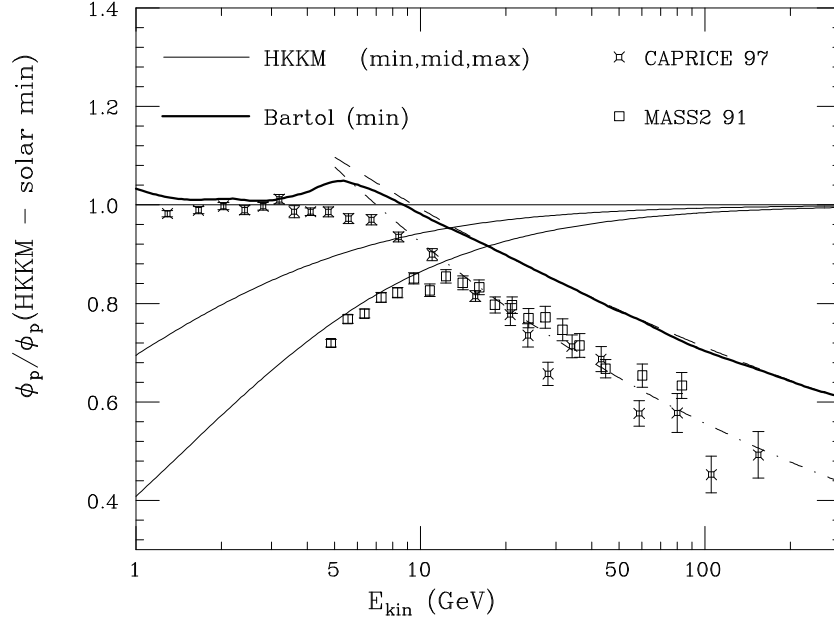


Fig. 6. Comparison of measurements of the primary c.r. flux and representations used in calculation of the ν -fluxes (see text).

flux and the solar activity is shown in fig. 7. The intensity of the cosmic rays at the Earth in the energy region $E_0 \sim 1\text{--}20$ GeV can be continuously studied at ground level using neutron monitor detectors. These detectors measure the hadronic component of secondary cosmic rays, detecting the neutrons produced in the interactions of the secondary particles in the material (lead) that surrounds the detector. The neutrons are moderated (with paraffin or polyethylene) and are detected as thermal particles using Boron tri-fluoride proportional counters. The rate measured by a neutron-monitor detectors depends on the magnetic latitude of the detector that determines the minimum rigidity of the primary particles that can reach the ground level, and by the altitude of the detector, that determines the absorption of the secondary particles. The top panel of fig. 7. shows the monthly average of the Sunspot Number since 1970, the bottom panel shows the variations in the monthly counting rate of three neutron monitors²⁹. The two thin histograms that shows a stronger variability give the activity measured by two detectors located at Kiel (altitude 54 meters, vertical cutoff 2.36 GV) and Moscow (altitude 200 meters, vertical cutoff 2.43 GV). The two histograms are nearly superimposed showing excellent correlation, they are measuring real variations of the primary c.r. flux. The thick histogram exhibiting a smaller variation is the activity measured at Huancaayo (Peru) (altitude 3400 m, cutoff Rigidity 12.92 GV). It can be seen how the time variability of the cosmic ray

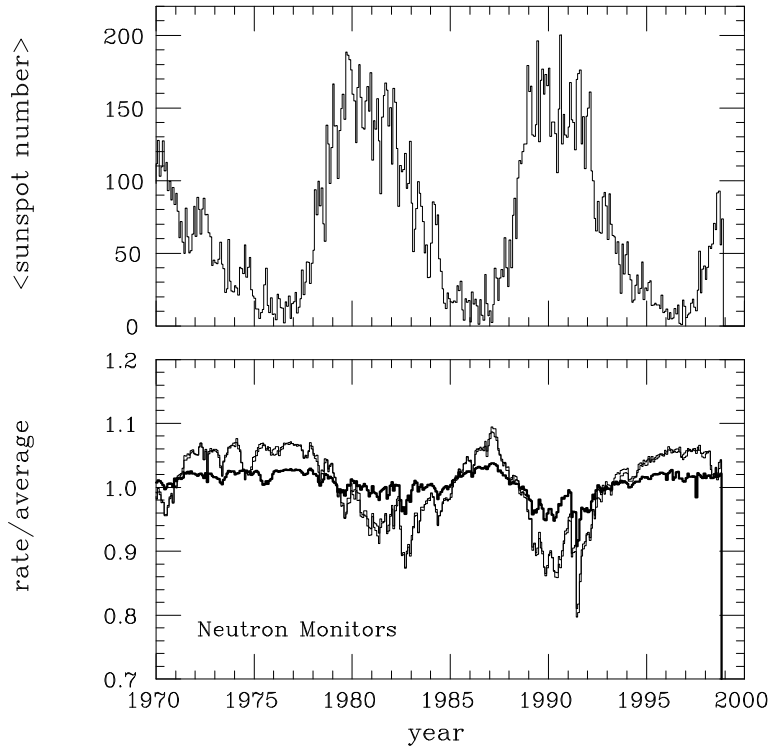


Fig. 7. The top panel shows the monthly average of the Sunspot Number. The bottom panel shows the relative rate of three neutron-monitor detectors, Kiel, Moscow and Huancayo (see text).

flux is reduced to less than 5% for this higher rigidity cutoff.

4.2. Geomagnetic effects

The geomagnetic field has some very important effects on the propagation of cosmic rays, and forbids low rigidity particles from reaching the surface of the Earth. The geomagnetic effects depend strongly on the position on the Earth of the observer, and on the direction of observation. For a qualitative understanding let us approximate the Earth magnetic field as a dipole, and consider two observers, the first at one magnetic pole, and the second on the magnetic equator. The ‘pole observer’ looking vertically up, can observe particles of all momenta, since in this case the field \vec{B} and the particle momentum \vec{p} are parallel and there is no bending of the particle trajectories; the observer located at the equator when looking for particles arriving horizontally from east can detect protons (or particles with charge $+e$) only if they have a momentum larger than approximately 59 GeV. Particles with this charge and momentum have an (unstable) circular trajectory that remains at a constant radius $r = r_{\oplus}$ seeing a magnetic field of constant intensity ($|\vec{B}| \simeq 0.31$ Gauss) always orthog-

onal to their 3-momentum. It is obvious that particles with lower momentum have ‘impossible’ trajectories. With a little more work one can calculate for example that the ‘equatorial observer’ looking horizontally west (vertically up) can observe protons with momentum $p \gtrsim 10$ GeV ($p \gtrsim 15$ GeV). In general for a detector position and direction of observation (\vec{x}, Ω) , it is possible to compute a ‘cutoff rigidity’ $R_c(\vec{x}, \Omega)$ ($0 \lesssim R_c \lesssim 59$ GV) such that only particles with $R \geq R_c$ can be measured.

The Liouville theorem states that the density of points in phase space volume is constant. This fundamental theorem has a simple and important application³⁰ to the propagation of cosmic rays in a static magnetic field. Since the momentum of the particles does not change in absolute value, then the differential flux along a particle trajectory is constant, and it follows that if the flux is isotropic at large distances from the Earth, then the flux in a small cone around any trajectory is constant and independent from the position. More formally if $\phi_\infty(p)$ is the isotropic flux at large distances from the Earth, then the flux measured by a detector at a point \vec{x} in the direction Ω has the form:

$$\phi_{\vec{x}}(p, \Omega) = \phi_\infty(p) \times \zeta(p, \Omega, \vec{x}) \quad (7)$$

where the quantity ζ is either 0 or 1, but never something else. The cosmic ray energy spectrum is therefore not deformed by the geomagnetic field and the effect of \vec{B}_\oplus is to ‘remove’ a set of momenta from the spectrum. In summary the calculation of the geomagnetic effects, using the facts that field \vec{B} is approximately constant in time and the primary flux is isotropic at large distances, can be reduced to the calculation of the allowed and forbidden trajectories.

This problem can be solved analytically for the special case of a volume that is entirely filled with an exactly dipolar magnetic field. In this case the function ζ has the form of a single sharp step^{31,32}. Introducing the rigidity $R = p/q$ the solution is:

$$\zeta(R, \Omega, \vec{x}) = \Theta[R - R_S(r, \lambda, \theta, \varphi)] \quad (8)$$

where $\Theta(x)$ is the Heavyside function ($\Theta(x) = 0$ for $x < 1$, $\Theta(x) = 1$ for $x \geq 1$), r is the distance from the dipole center, λ is the magnetic latitude, θ is the zenith angle, φ is the azimuth angle measured clockwise from the magnetic north, and R_S is the Störmer³¹ rigidity cutoff that for positively charged particles is:

$$R_S(r, \lambda, \theta, \varphi) = \left(\frac{M}{2r^2} \right) \left\{ \frac{\cos^4 \lambda}{[1 + (1 - \cos^3 \lambda \sin \theta \sin \varphi)^{1/2}]^2} \right\} \quad (9)$$

(for negatively charged particles the cutoff is obtained with the reflection $\varphi \rightarrow \varphi + \pi$) that is exchanging east and west). In (9) M is the magnetic dipole moment of field. For the Earth $M \simeq 8.1 \times 10^{25}$ Gauss cm³ that corresponds to a polar magnetic field of 0.62 Gauss. The quantity $M/2r_\oplus^2 \simeq 59.4$ GV corresponds to the rigidity of a particle in a circular orbit of radius r_\oplus in the earth’s magnetic equatorial plane.

The Störmer analytic result is only an approximation for a realistic calculation because of two effects: (i) the Earth field is not exactly dipolar, (ii) the field does not fill the entire space, and therefore a fraction of the trajectories that are ‘allowed’ according to the Störmer formula intersects the surface of the Earth and is in fact forbidden. The problem can be solved in general numerically using the backtracking method. In this method to determine if a cosmic ray trajectory (\vec{x}, \vec{p}, q) is allowed or not, one integrates numerically the equation of motion for a particle of momentum $-\vec{p}$ and charge $-q$, starting from the point \vec{x} using a detailed description of the geomagnetic field, this of course corresponds to the calculation of the past-trajectory of the particle considered. If the trajectory ‘goes to infinity’ without intersecting the surface of the earth, the initial trajectory is allowed: $\zeta(\vec{p}, \vec{x}, q) = 1$. If the trajectory intersects the Earth, or remains confined within a finite radius the trajectory is forbidden: $\zeta(\vec{p}, \vec{x}, q) = 0$. We note that in the exact calculation the function $\zeta(R, \Omega)$ has not anymore the form of a single step function, and in a narrow range of p/q there are alternating intervals of allowed and forbidden rigidities (the ‘penumbra’ region), therefore strictly speaking for a fixed position \vec{x} and direction Ω one should not speak about a single cutoff rigidity but of a minimum allowed rigidity R_1 and a maximum forbidden rigidity R_2 (with $R_1 \leq R_2$), however since $R_1 \simeq R_2$ the concept of cut-off remains qualitatively useful. Both the Bartol³³ and HKKM¹⁰ calculations use the backtracking method to estimate the geomagnetic effects. An important confirmation of the correctness of the estimate of the geomagnetic effects has been obtained with the experimental observation of the east-west anisotropy for atmospheric neutrinos performed by SK¹⁵.

4.3. Isotropy of the c.r. flux

In the previous subsection we have assumed that the c.r. flux, in the absence of geomagnetic effects is isotropic. This ‘intrinsic’ isotropy can in principle be studied measuring the flux in a fixed direction in the detector system of coordinates so that the geomagnetic effects are constant. Since the Earth is rotating this allows to study the variations of the primary flux in a cone in celestial coordinates. The measurements for the range of primary energy of interest have shown the existence of ‘solar’ anisotropies (related to day–night effects) with amplitudes of a fraction of a percent and no ‘sidereal’ anisotropies³⁴.

5. Modeling of the development of hadronic showers

The modeling of the development of hadronic showers is a second important source of uncertainty in the calculation of the ν fluxes. A cosmic ray shower has a ‘tree’ structure and can be seen as made of branches and vertices. The primary particle interaction point is the first vertex of the tree, the secondary particles produced in

Fig. 8. From ¹⁹. Distributions of fractional momentum of π^\pm produced in the interactions of $\simeq 20$ GeV/c momentum protons with light nuclei obtained in three different models: Bartol (BGS)⁹, HKKM¹⁰ and Bugaev and Naumov¹¹ for hadronic interactions on an air target. The points are estimates obtained integrating on p_\perp The data on Beryllium³⁶.

this this interaction are a first set of branches. Each one of the secondary particles can be followed, taking into account energy loss, deviations in the geomagnetic field and multiple scattering, until the particle, decays, interacts, stops, or reaches the detector level. Decays and interactions can be seen as additional vertices, where one ‘in’ particle is destroyed and several ‘out’ particles (or new branches) are produced. The new particles can also be followed, and the process recursively iterated. The neutrinos are produced in the weak decays of kaons and charged pions. Because of this tree structure, the calculation of cosmic ray shower is a problem that can be solved in the most natural and accurate way with Montecarlo techniques. Analytic treatments are also possible^{11,35} and represent a reasonable approximation that allows to gain insight on the physics of the problem, however the MC methods are more general and precise and have to be preferred.

5.1. Modeling of the hadronic interactions

The main uncertainty in the modeling of hadronic showers is the description of particle production in hadronic interactions. The multiplicity, energy spectrum and flavor composition of the particles produced in the final state are all important factors in the determination of the ν fluxes.

In fig. 8 taken from¹⁹ a review paper on the calculation of atmospheric ν fluxes we show the energy distribution of charged pions produced in the interactions of 24 GeV protons on air as modeled in different calculation of the atmospheric ν fluxes. Inspection of fig. 8 shows that the Bartol calculation has a higher multiplicity and a slightly harder energy spectrum of the HKKM one, and much larger difference with respect to the Bugaev and Naumov estimates. This difference in the modeling of particle production would account for a $\sim 20\%$ difference in the ν event rate between the Bartol and HKKM calculation if the same primary flux is assumed.

A comparison of the FLUKA¹³ and Bartol⁹ interaction models, shows that the FLUKA code also predicts a smaller multiplicity for charged pions, this will result in a smaller ν flux for the same primary flux. The details of the full calculation will soon be made available.

5.2. The method of calculation: 3D versus 1D

The MC calculation of an hadronic shower is in principle a straightforward, even if technically not trivial, computational problem. All the physics that is needed is

well known, with the only exception of the description of the hadronic cross sections, discussed in the previous subsection. However all the calculations that are publicly available (with the exception of a first attempt by Lee and Koh¹²) have been made in the approximation of considering the development of the hadronic showers as one-dimensional. This implies (discussing in particular the implementation of the approximation in the Bartol code) the following: (a) multiple scattering and deviations in the magnetic field are neglected: all particles propagate along straight lines; (b) in the generation of the interaction or decay vertices the kinematical properties of final state particle are calculated exactly including the generation of p_\perp and the exact conservation of 4-momentum, however after the generation of the vertex is completed, for all particles with $p_\parallel > 0$ the angle with respect to the primary particle is set to zero while particles with $p_\parallel < 0$ are disregarded. In this way each ν is exactly collinear with its primary particle.

The motivations for this approximation are purely technical: the saving of computer time. The neutrinos that reach a detector in a certain geographical position (say Super-Kamiokande) are in general produced in cosmic ray showers that developed anywhere on the earth and (allowing for ν 's non collinear with the primary particle) with any direction. It is clear that the Montecarlo generation in this general scheme is very inefficient, because one has to generate *all* possible cosmic ray showers in the Earth atmosphere, but only a very small fraction of them will produce neutrinos in the vicinity of the detector. With the assumption of collinearity only a very small subset of the cosmic ray has to be studied and the problem becomes numerically enormously simpler.

The dominant contribution to the angle $\theta_{0\nu}$ between the neutrino and the parent particle arises because of the non-collinearity of the parent mesons with the primary particle, and (for ν from muon decay) because of the deviation of the μ^\pm is the geomagnetic field with the $\pi\nu$ angle a smaller contribution:

$$\langle\theta_{0\nu}\rangle \simeq \theta_{0\pi} \oplus \theta(\mu^\pm, B_\oplus) \simeq \frac{\langle p_{\perp\pi} \rangle}{p_\pi} \oplus \left(\frac{L_\mu B_{\oplus\perp}}{p_\mu} \right) \sim \frac{4.3^\circ}{E_\nu(\text{GeV})} \oplus \frac{10^\circ}{E_\nu(\text{GeV})} \quad (10)$$

A first test of the importance of 3D effects in the calculation of the atmospheric ν fluxes has been performed with FLUKA¹⁴. The test is a comparison of two calculations of the ν -fluxes performed with the 1D approximation or with a fully 3D method, but in both cases assuming spherical symmetry for the Earth and the absence of the geomagnetic field. In this approximation, all points on the surface of the Earth are equivalent and can be considered as a single detector, therefore the CPU time problem is not present, note however that since the deviation of the muons in the geomagnetic field is neglected, the angle between ν and primary particle is underestimated. The results of the test show that the effects of the 1-dimensional approximation are negligible for multi-GeV events, and a small correction for sub-GeV events. A complete 3D calculation is feasible using an efficient weighting of the simulated events. Results

on fully 3D calculations of the ν fluxes should very soon be made publically available (at least) from the Fluka and Bartol groups.

5.3. *The density of the atmosphere and the mountains*

The density of the medium where the c.r. shower develops, changes with continuity and it is essential to take this fact into account. The density profile of the atmosphere can to a good approximation be taken as constant in time and independent of position (the concept of altimeter is based on this approximation). Variations of the average density profile with the geographical latitude and the season have been investigated and are the source only of minor corrections for low energy neutrinos. For accurate calculations it is also necessary to consider the profile of the mountains above the detector. This is straightforward to do, and represents a few percent reduction of the component of high energy and vertical down-going neutrinos that is produced in muon decay, the effect is therefore stronger for electron neutrinos.

6. The neutrino cross section

The description of the neutrino cross section is a source of uncertainty of comparable importance to the primary flux and the hadronic cross sections in the prediction of the atmospheric ν event rates. At high E_ν , when most of the phase space for ν interactions is in the deep-inelastic region, σ_ν is reliably calculable in terms of well determined parton distribution functions (PDF's). However in the energy range relevant for atmospheric neutrinos ($E_\nu \sim 1$ GeV) the description of σ_ν is theoretically more difficult, and the available data is not sufficient to constrain the cross section to better than 15–20%.

Quasi-elastic scattering is the most important mode, its importance being enhanced by the event selection criterion (the ‘single ring’ condition) that requires a single visible particle in the final state. Uncertainties on this process arise from uncertainties in the axial form factor of the nucleons (that cannot be measured in electron scattering), and more important from the description of the nuclear effect corrections. Most MC codes use some version of the Fermi gas model³⁷. More sophisticated studies^{38,39} have attempted to calculate the nuclear effects beyond the Fermi gas model using different theoretical methods to describe the nuclear medium. These studies were originally developed to see if nuclear effects could somehow result in different cross section for ν_e 's and ν_μ 's, and so explain the low (μ/e) ratio observed experimentally. No such flavor dependence has been found, however the calculations have also estimated significant effects (10–15%) in the absolute value of the QE cross sections. The Soudan detector in a good fraction of the events can measure together with the charged lepton, also the recoil proton in processes as: $\nu_\mu Fe \rightarrow \mu^- p A^*$, where A^* is an undetected nuclear system. The resolutions that can be attained for the neutrino

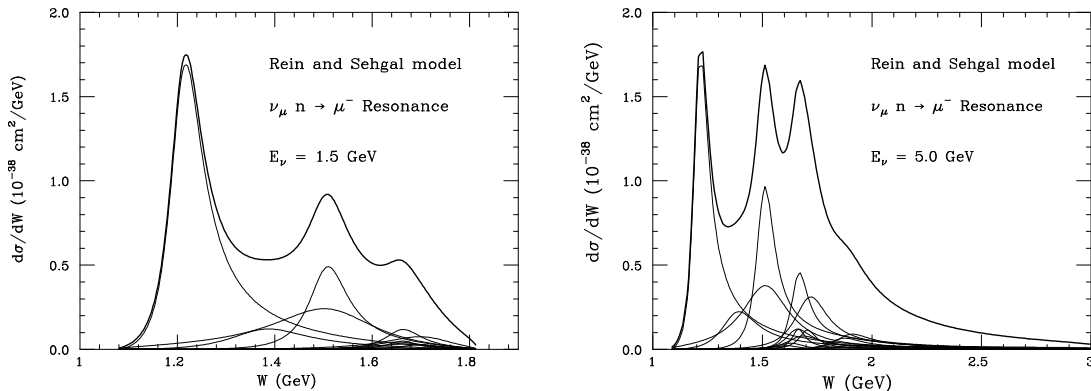


Fig. 9. Differential cross section $d\sigma/dW$ for the scattering $\nu_\mu n \rightarrow \mu^- R$ where R is a baryonic resonance, calculated according to⁴⁰. The thick curve is the sum of all contributions.

kinematical properties (E_ν and Ω_ν) depend on how much 4-momentum is carried away from the undetected nuclear system (the ‘spectator’ in the simple Fermi gas model), and can depend on the modeling of the nuclear effects. A detailed study should investigate if the resolutions estimated in the Fermi gas model⁵ are correct.

Processes where the target nucleon is excited to a resonance are also of great importance in the energy region relevant for atmospheric neutrinos. Both the Super-Kamiokande and Soudan MC codes describe this cross section using the algorithms of Rein and Sehgal⁴⁰ that apply to neutrino interactions the model of baryonic resonances of Feynman, Kislinger and Ravndal⁴¹ that describes the baryons as bound states of three valence quark in an harmonic oscillator potential. Two examples of the prediction for $d\sigma/dW$ (W is the mass of the hadronic system in the final state), calculated according to the original work, are shown as an illustration in fig. 9. We note that the Rein and Sehgal model predicts a complex structure in the W distribution, and at intermediate energy not only the Δ resonance (the strongest peak at $W \simeq 1.232$ GeV) but also other states give important contribution to the cross section. The existing data does not give a clear confirmation of the prediction. Nuclear effects are also important for resonance production. In particular in a nuclear medium there is the possibility of a baryonic resonance that is dis-excited to a nucleon, with the scattering appearing experimentally as QE scattering.

All other channels in the ν cross section are usually described using the standard expression for deep inelastic scattering (DIS)⁴². In fig. 10 we show examples of the differential cross sections $d\sigma/dW$ and $d\sigma/d\ln Q^2$ calculated using the DIS formulae, and the leading order PDF’s of GRV94⁴³. Looking at $d\sigma/dW$ in the left panel of fig. 10 one can see that as expected the DIS formula does not ‘know’ anything about the hadronic mass spectrum, so it does not describe resonances and in fact it computes a cross section also in the unphysical region $m_p < W < (m_p + m_\pi)$ that is forbidden because no hadronic state with mass in this interval can exist. It remains an open problem how to ‘join’ smoothly the baryon resonance production with the

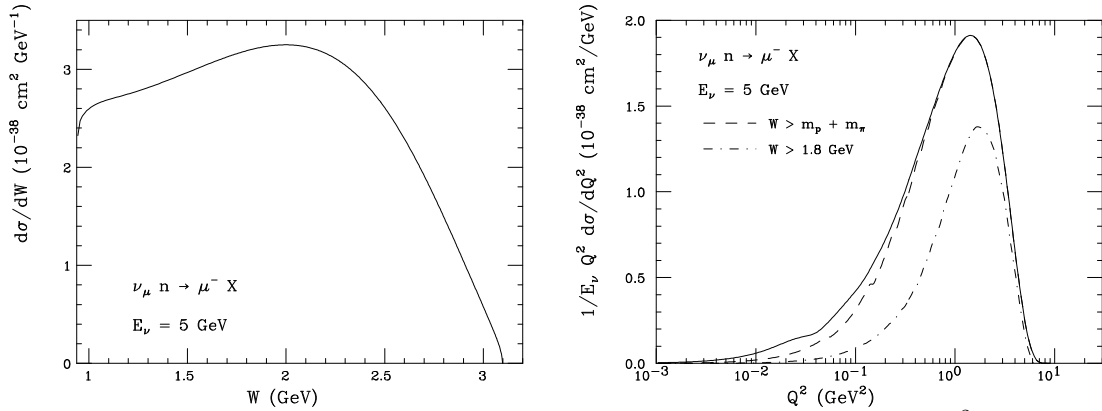


Fig. 10. Left: plot of $d\sigma/dW$ for $\nu_\mu n \rightarrow nX$ interactions. Right: plot of $d\sigma/d\ln Q^2$ for the same reaction. The ν cross section is calculated using the DIS formulae and the GRV94LO PDF's.

all other channels described collectively by DIS. It should also be noted, that because of the low energy of atmospheric ν 's the Q^2 in the interactions is always small, even if the final state hadronic system is excited above the resonance region (see the right panel of fig. 10) and therefore the use of the DIS framework is not on a solid ground.

The importance of the neutrino cross section in the prediction of the atmospheric neutrino event rates is revealed by the effect of a relatively small modification of the description of σ_ν in the SK Montecarlo: the choice of a new set of PDF's (GRV94LO⁴³ replacing the CCFR parametrization) to describe the DIS part of σ_ν . Combined with the use of the medium solar activity ν fluxes of HKKM¹⁰ (that has a small impact for multi-GeV events) has led for example to an increase of 4% (8%) for the μ -like (e -like) fully contained events, and 7% for the partially contained events (compare the MC predictions in¹ and²).

It appears very difficult to calculate accurately σ_ν from first principles in the relevant energy region. The existing data do not determine the absolute value of σ_ν and the energy spectrum of the final state lepton better than $\sim 15\%$. A significant improvement can probably only be obtained with the analysis of more data. The K2K long-baseline ν beam⁴⁴ with a spectrum not too different from the atmospheric one offers very interesting possibilities. The placement in the 'near' position along the beam of detectors with higher resolution and/or an iron or argon target could also be useful for a more complete study.

One final remark on the question of the ν cross section, is that all the experimental groups that have made measurements of atmospheric ν 's have compared their results to predictions calculated using different descriptions of σ_ν and different MC codes (in general not publically available) for the generation of the ν interactions. A detailed comparison of the descriptions of σ_ν used by the different groups is missing. This lack of information can be a source of confusion. For example it is important to understand the reasons for the difference in the ratios $e_{\text{data}}/e_{\text{MC}}$ stated by the SK

and Soudan (see section 8) and establish it is due to the ν flux or, at least in part, to different assumptions about the ν cross sections.

7. The muon flux constraints

The fluxes of atmospheric muons are strictly related to the neutrino ones, because almost all ν 's are produced either in association with, or in the decay of μ^\pm . Precise measurements of the muons offer then a way to check directly the ν fluxes. To constraint the flux of neutrinos with energy E_ν , the most interesting muons are those created with energy around $E_\mu \sim 2 E_\nu$ (the factor of two being a kinematical effect). The most important range of ν energy is $E_\nu \sim 0.1\text{--}10$ GeV, and especially for the lowest part of this range, only a vanishing or small fraction of the related muons reach the ground because of energy loss (the atmosphere corresponds to a loss of ~ 2 GeV for a vertical muon) and decay (the μ decay length is $\ell_\mu \simeq 6.2 p_\mu(\text{GeV})$ km). For low energy muons the measurement is possible only at high altitude.

The authors of the existing atmospheric ν calculations checked that their predictions for the muon flux (that is ‘automatically’ calculated together with the ν flux) with the existing muon data^{45,46} at ground level. To a large extent the agreement between the HKKM and Bartol calculations of the ν fluxes, that is the effect of a cancellation between different estimates of the primary flux and different modelings of the hadronic interaction, is not casual, but the result of the μ constraint. Recently new measurements^{47,48,26} of the ground level muon flux, have been performed with detectors developed for balloon flights. The new data suggests that previous estimates could be too high, (see for example fig. 11). This is an important point that need to be studied in detail. New precision measurements of muons at ground level in sites with different geomagnetic cutoffs and at different altitudes would certainly be very valuable.

In recent years, the balloon detectors have performed measurements of the muon spectrum during their ascent in the atmosphere^{49,50,51,52}. The analysis and discussion of these results is still in progress. Preliminary comparisons of these results with MC calculations have shown some significant discrepancies (especially for $E_\mu \lesssim 1$ GeV) that require a more detailed study. These are difficult measurements, with the altitude of the detector continuously varying, and the statistical errors are still large because of the short time available during balloon ascent, some discrepancies between the results of different groups do exist, however these and future measurements at high altitude (with detectors on balloons or possibly airplanes⁵³) have a good potential for reducing the uncertainties in the flux of atmospheric neutrinos.

8. The ‘Normalization problem’

In the analysis of their data the SK and Soudan collaboration consider the absolute

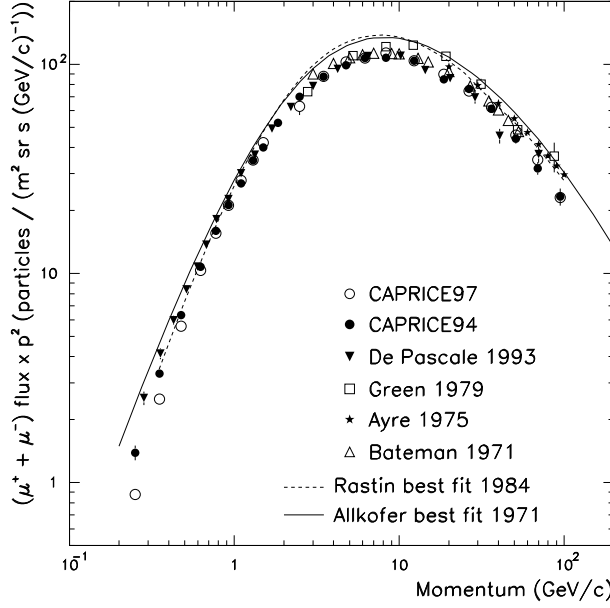


Fig. 11. Flux of muons at the ground measured by the Caprice detector⁴⁸, compared with fit to previous data.

normalization of the calculated ν fluxes as a free parameter. In the SK analysis of the data in term of $\nu_\mu \leftrightarrow \nu_\tau$ oscillations, the ν fluxes are fitted to the form

$$\begin{aligned}\phi_{\nu_\mu}(E_\nu, \theta_z) &= (1 + \alpha) \phi_{\nu_\mu}^{\text{th},0}(E_\nu, \theta_z) \langle P_{\nu_\mu \rightarrow \nu_\mu}(E_\nu, \theta_z; \sin^2 2\theta, \Delta m^2) \rangle \\ \phi_{\nu_e}(E_\nu, \theta_z) &= (1 + \alpha) \phi_{\nu_e}^{\text{th},0}(E_\nu, \theta_z)\end{aligned}\quad (11)$$

where $\phi_{\nu_\mu(\nu_e)}^{\text{th},0}$ are the published no-oscillation fluxes of HKKM (or Bartol) and α is an unconstrained normalization parameter. In the analysis of 535 days live days of SK, for the best fit point, the normalization parameter had the value $\alpha = +0.158$, also the ratios $e_{\text{data}}/e_{\text{MC}}$ for the sub-GeV and multi-GeV samples. had the values 1.18 ± 0.03 and 1.23 ± 0.07 (statistical errors only). In other words according to the analysis in¹ the the calculated ν fluxes of Honda et al.¹⁰ are too low by $\sim 15\text{--}20\%$. This result is within the stated uncertainty in the absolute normalization of the calculation, however since the primary c.r. flux used in the HKKM calculation is likely to be too large, this relatively high measured neutrino rate has generated discussions and speculations, at least in part motivated by the observation, that under the hypothesis of $\nu_\mu \leftrightarrow \nu_\tau$ oscillations the flux if electron neutrinos is not affected by oscillations, however is $\nu_\mu \leftrightarrow \nu_e$ transitions exist, it can be enhanced.

In the analysis of 735 days presented at this conference the SK collaboration estimates a lower normalization parameter $\alpha = 0.084$. This can also be seen observing that the ratios $e_{\text{data}}/e_{\text{MC}}$ take the new values 1.06 ± 0.03 and 1.08 ± 0.05 (for sub-GeV and multi-GeV). The significant differences with respect to the previous analysis are

due to a combination of changes in the MC predictions and of statistical fluctuations in the data.^c The MC prediction has increased because of two effects: (i) the data is compared to the ν fluxes of HKKM calculated for minimum solar activity, while in the 545 days analysis¹ the data was compared to medium solar activity;^d (ii) the description of the ν cross section has been modified as discussed in section 6 with a resulting enhancement of the event rate. The combined effects of these changes are an enhancement of the MC rate of 4% (8%) for the sub (multi)-GeV sample.

The result of the Soudan-2 experiment⁵ for the ‘shower’ events is $e_{\text{data}}/e_{\text{MC}} = 0.81 \pm 0.09$, for all contained events, (0.86 ± 0.11 for the ‘high resolution sample’) that is an effect of opposite sign with respect to SK. In this case the MC calculation is based on the Bartol⁹ ν fluxes. The difference in $e_{\text{data}}/e_{\text{MC}}$ between SK and Soudan is a hint of a possible problem, and should be carefully investigated. The neutrino flux at Soudan is softer than at Kamioka (see fig. 3) and is produced on average by lower energy primaries (see fig. 4), therefore the difference between the estimated ratios $e_{\text{data}}/e_{\text{MC}}$ at Kamioka and Soudan is not necessarily an experimental discrepancy, but it could be for example an indication that the calculated ν flux is too soft. In section 8, we will discuss the possible effects of a modification of the shape of the ν energy spectra.

9. Determination of the oscillation parameters

In this section I will try to illustrate (only qualitatively) possible effects of the uncertainties in the predictions of the ν event rates in the determination of the oscillation parameters in the hypothesis of the existence of $\nu_\mu \leftrightarrow \nu_\tau$ oscillations.

9.1. The Soudan experiment

The Soudan experiment⁵ has measured for the ‘high resolution sample’ a double ratio $R = 0.59 \pm 0.09$. This value is obtained as: $0.59 = 0.74/1.25$. It is important to note that the denominator of the double ratio $(\mu/e)_{\text{MC}}$ is significantly smaller than the naive expectation of approximately two.^e The low value of $(\mu/e)_{\text{MC}}$ can be easily understood as the consequence of different detector efficiencies for μ -like and

^c The difference in the estimates of the rate of sub-GeV e -like events for the 535 and 736 days analysis has generated speculations⁵⁴ that the ν fluxes have a time varying component. The analysis in⁵⁴ does not take into account small modifications of the pattern reconstruction program that affect the entire integrated data sample. Taking this into account, the evidence for a transient component in the ν flux becomes much weaker.

^d The use of the solar minimum fluxes is certainly well motivated considering the solar activity during the data taking period (see fig. 7), the higher p flux implied by this assumption could however be in worst agreement with the most recent data (see fig. 5) on the primary c.r. flux.

^e The same argument is also valid for the single track/shower events, where the double ratio is $R = 0.66 \pm 0.11$, with $0.66 = 0.70/0.95$

e -like events. Muons are more penetrating than electrons, and the containment requirement results in a reduced efficiency for higher energy muons, and therefore in a low value for the μ/e ratio. This implies that the (μ/e) ratio is sensitive to the *shape* of the ν energy spectrum with a softer (harder) spectrum resulting in a higher (lower) ratio. If the calculated ν flux (as an example) falls more steeply with energy than the true spectrum, the denominator of the double ratio is overestimated, therefore R is underestimated and the estimate of the oscillation parameters is biased: for a fixed value of $\sin^2 2\theta$, the range of allowed $|\Delta m^2|$ is overestimated.

As discussed in section 7, there is some experimental indication that the shape of the ν energy spectrum is not predicted correctly because the measured event rate for sub-GeV e -like events in Soudan is 15–20% lower than the prediction, while in Super-Kamiokande, where $\langle E_\nu \rangle$ is higher because of different geomagnetic effects, the detected rate is 6–8% higher than the prediction. If this is interpreted as evidence that the ν spectrum is flatter than the prediction, the allowed region for $|\Delta m^2|$ estimated by Soudan should be revised to lower values.

The Soudan experiment, differently from SK, has *not* observed a clear zenith angle modulation of the μ -like event rate. This can be interpreted as an indication that the ν oscillation length is sufficiently short, so that also down-going ν_μ are significantly suppressed by oscillations, and can be used to exclude low values of Δm^2 . This conclusion is also somewhat model dependent, because for the low energy ν 's detected by Soudan, the geomagnetic effects induce a non negligible up-down asymmetry, with an excess of up-down events. The ‘geomagnetic asymmetry’ has to be subtracted from the data in order to put in evidence the possible suppression of up-going neutrino induced by oscillations. From table 2 we can see for example that the Bartol prediction for the ‘geomagnetic asymmetry’ at Soudan depends on the solar cycle epoch and decreases for the flatter spectrum of solar maximum activity. Therefore a flatter neutrino energy spectrum⁵⁵ would predict of a smaller asymmetry induced by geomagnetic effect, then the experimentally detected asymmetry (that is of order $A = -0.25 \pm 0.16$) would be interpreted as more significant, and again the allowed interval for $|\Delta m^2|$ for the $\nu_\mu \leftrightarrow \nu_\tau$ hypothesis would be shifted to lower values.

9.2. The Super-Kamiokande experiment

In the case of the Super-Kamiokande experiment, the up-down asymmetry represents really a ‘smoking gun’ evidence for new physics. The theory predicts unambiguously that at Kamioka the up-down asymmetry is *positive* (excess of up-going particles) and of order $A \simeq 0.01$ for the multi-GeV events. The detected asymmetry becomes more pronounced with increasing energy, precisely as expected considering the improving correlation between neutrino and muon direction, and the shape of the distortions of the zenith angle distributions also match very well the expectations. As

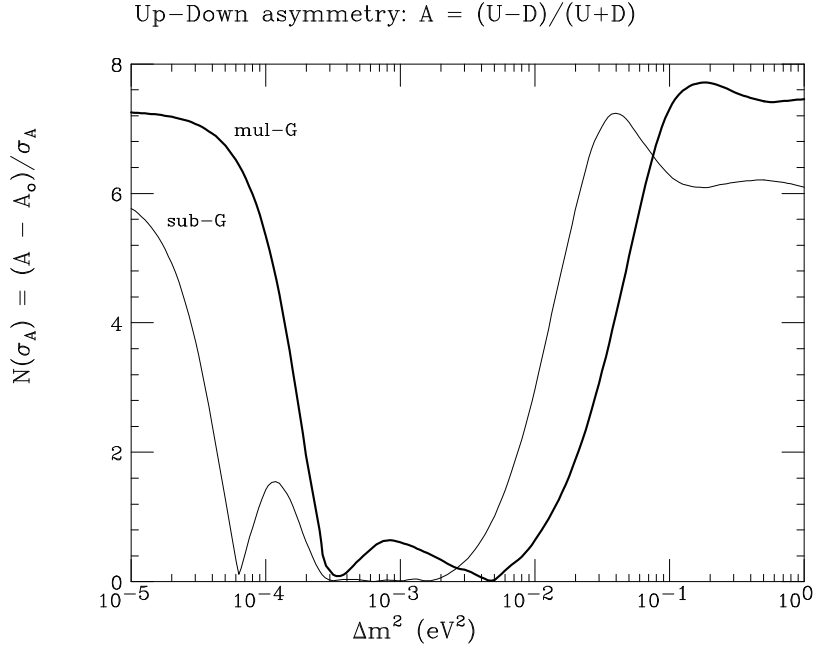


Fig. 12. Number of standard deviations for the Up/Down asymmetry measured by SK. The two curves are for sub-GeV and multi-GeV data.

a consequence, the possibilities of a very large difference in acceptance for up-going and down-going particles, or of the presence of a very large non-neutrino background appear extremely contrived and unlikely.

The up-down asymmetry of multi-GeV events is an excellent method to measure the mixing parameter $\sin^2 2\theta$. Since the pathlength for neutrinos coming from vertically up or down differ by three orders of magnitude, it can be expected that for a broad range of $|\Delta m^2|$, if the correlation between the ν_μ and the detected μ directions is good, one will have that oscillations are absent for down-going particles and can be averaged for up-going particles. Selecting two cones around the vertical, it is natural to expect that $U \simeq U_0 (1 - \sin^2 2\theta/2)$, and $D \simeq D_0 \simeq U_0$. The mixing parameter can then be determined independently from the squared mass difference as $\sin^2 2\theta = 2(1 - U/D)$ with a precision that is essentially limited by the statistical errors. Using this ‘algorithm’ the SK result for the asymmetry for the multi-GeV data: $A = -0.31 \pm 0.04$ can be translated in a measurement of the mixing parameter $\sin^2 2\theta = -4A/(1 - A) = 0.95 \pm 0.09$, a result in good agreement with what is obtained in the detailed fit.

This argument however tells us that the up-down asymmetry is not a good quantity for the measurement of Δm^2 . This is illustrated in fig. 12 that shows as a function of $|\Delta m^2|$ the number of standard deviations of the asymmetry measurement for the sub-GeV and multi-GeV sample from predictions calculated assuming the presence of $\nu_\mu \leftrightarrow \nu_\tau$ oscillations with maximal mixing. The shapes of the curves show that there is a broad interval of $|\Delta m^2|$ where the asymmetries have the measured value.

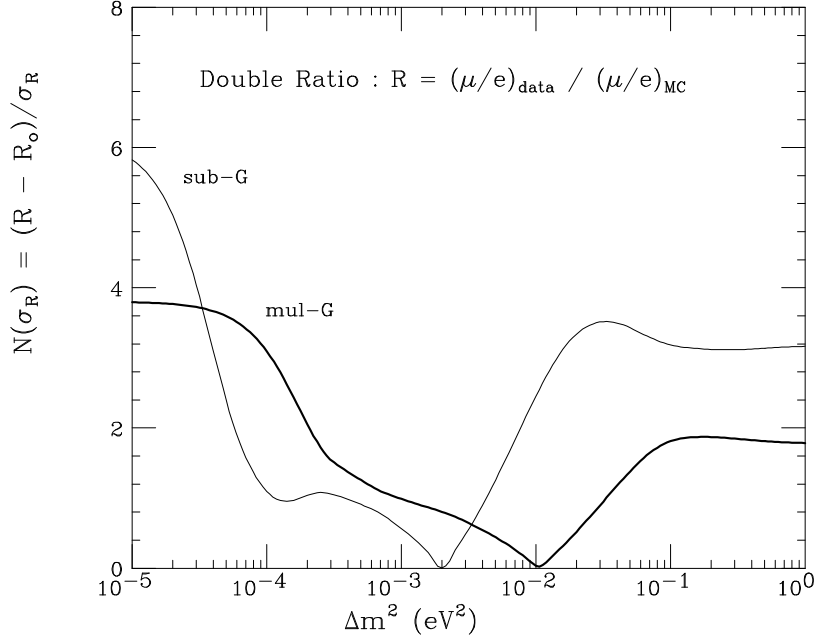


Fig. 13. Deviations (in standard deviations) of the measured SK sub-GeV and multi-GeV double-ratios with respect to expectations calculated assuming the presence of maximal mixing $\nu_\mu \leftrightarrow \nu_\tau$.

In fig. 13 we show as a function of $|\Delta m^2|$ the deviations of the (μ/e) double ratios for the SK sub-GeV and multi-GeV data with respect to the prediction made assuming again the presence of $\nu_\mu \leftrightarrow \nu_\tau$ oscillations with maximal mixing. To compute the number of standard deviations the value of σ_R has been estimated combining in quadrature the statistical errors with the systematic uncertainty as given by SK. The shape of the curves in fig. 13 are qualitatively easy to understand, the suppression of the μ -like events grows monotonically from zero for very small $|\Delta m^2|$ when no neutrinos has time to oscillate, to 0.5 at large $|\Delta m^2|$, when the effect of rapid oscillations can be averaged. Since the oscillation probability is a function of $|\Delta m^2|/E_\nu$, and the measured double ratios for the sub-GeV and multi-GeV are approximately equal (0.67 and 0.66), the curve for the multi-GeV data that describes the suppression of higher energy neutrinos, is shifted to higher values of $|\Delta m^2|$. Comparing fig. 12 and fig 13 one can see that the lowest value of $|\Delta m^2|$ of an allowed interval for SK is determined by the measurement of the double ratio for multi-GeV events.

As in the case of Soudan, the analysis of the double ratio is model dependent, because since the e -like and μ -like events are produced by different ranges of E_ν , different assumptions for the shape of the neutrino energy spectrum result in different predictions for the (μ/e) ratio, and therefore to different interpretations of the experimental results. In fig. 14 shows the approximate energy distributions of the neutrinos that produce different event samples in SK. It is instructive to observe that because

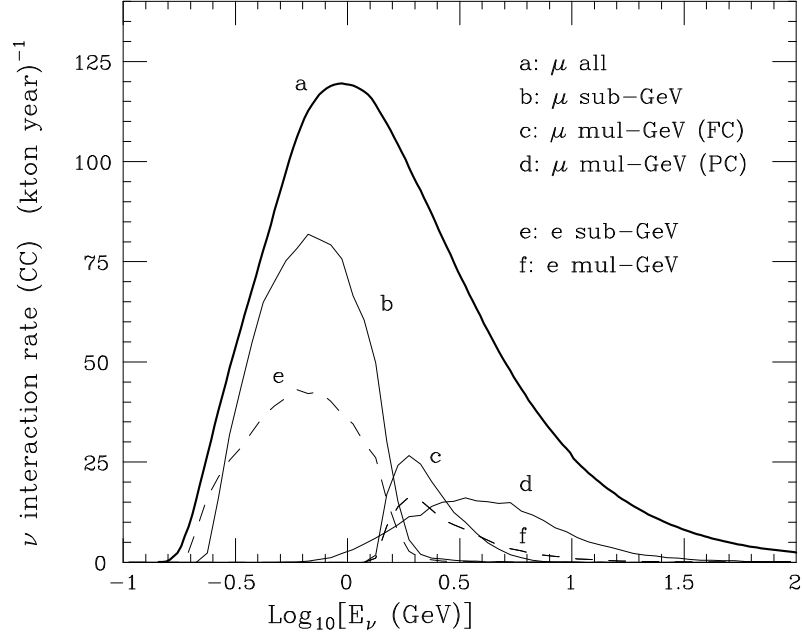


Fig. 14. Approximate energy distributions of interacting neutrinos for different classes of events in SK. Note the difference in the shape of the response for μ -like and e -like events.

of the containment requirement, in the the multi-GeV sample fully contained (FC) e -like events have a broader energy distribution (extending to higher E_ν) than FC μ -like events, and in fact the MC double ratio for these events is 1.16 (significantly smaller than two). However μ -like events are also detected as partially contained (PC) events. For this class of events the single ring requirement that is an important source of inefficiency for large E_ν when the average multiplicity grows, is removed. For this reason the PC events are produced by a still broader range of E_ν that extends beyond the energy interval for e -like events.

This question is illustrated with a ‘pedagogical example’ in fig. 15. In this figure we have performed three Montecarlo simulations of the SK data that differ only for the description of the neutrino spectrum. One calculation uses the standard solar minimum HKKM fluxes, while the other two assume a flattening (steepening) of both ν_e and ν_μ fluxes with a large distortion factor $\propto E_\nu^{\pm 0.03}$ (the absolute normalization has no importance in this analysis). The spectral distortion has a negligible effect on the (μ/e) ratio at a *fixed* E_ν , but has a significant impact on the predicted ratio for the rates for the entire multi-GeV sample because of the different energy dependence of the detection efficiency for the two flavors. The flatter spectrum predicts a larger no-oscillation (μ/e) ratio, and in the interpretation of the data in terms of $\nu_\mu \leftrightarrow \nu_\tau$

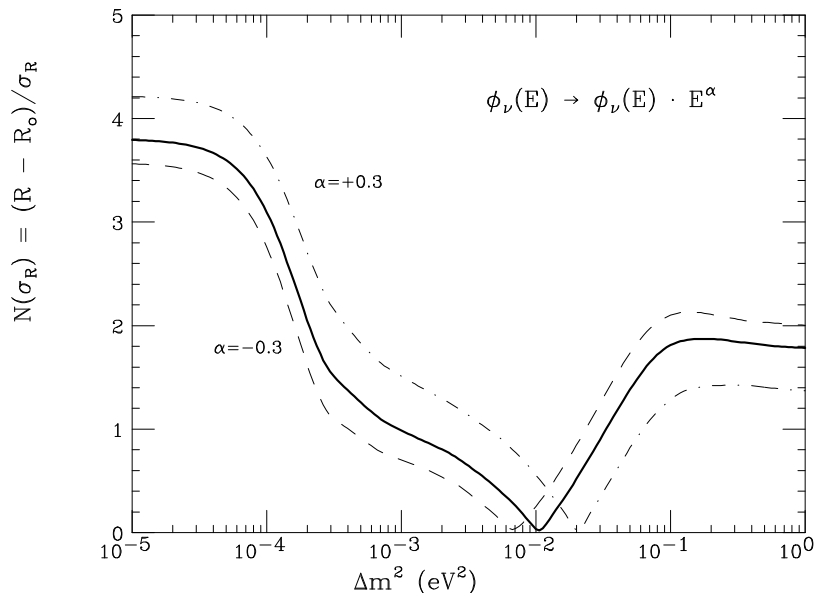


Fig. 15. Deviation (in standard deviations) of the measured SK multi-GeV double-ratio with respect to an expectation calculated assuming the presence of maximal mixing $\nu_\mu \leftrightarrow \nu_\tau$. The dashed and dot-dashed curve are calculated assuming a distortion of the HKKM ν fluxes.

oscillations results in a larger $|\Delta m^2|$ to explain the larger suppression.^f

10. Summary

The evidence for the disappearance of ν_μ 's in the atmospheric neutrino data is robust, and represents a very important result. The detailed interpretation of the experimental results is limited by systematic uncertainties in the prediction of the event rates.

One of the main sources of uncertainty related to the spectrum of primary cosmic rays, has been significantly reduced thanks to new measurements with detectors on balloons. One more measurement of the primary fluxes of the Anti Matter Spectrometer (AMS) should soon become available. This new information on the primary fluxes has not yet been included in the simulations.

Uncertainties in the modeling of particle production in hadronic interactions is now probably the most important limitation in the calculation of the atmospheric ν fluxes. New measurements of the properties of particle production in proton-nucleus interactions in the energy range $E_{lab} \sim 3\text{--}100$ GeV could significantly reduce the systematic error in the prediction of the normalization and energy spectrum of

^fAn additional effect is also that for a flatter spectrum, the average energy of the neutrinos that produce the events in the sample is higher and therefore even to produce the same average suppression, the $|\Delta m^2|$ must be larger.

the atmospheric ν -fluxes. The improvement in the determination of the primary flux makes this experimental program more attractive and useful because a better determination of the hadronic cross sections can now be directly translated in an improvement in the determination of the atmospheric ν -fluxes.

The neutrino cross section has also to be recognized as an important source of systematic uncertainty, also relevant for the LBL disappearance programs. The best perspectives for improvement come again from the performance of new experiments.

Measurements of the muon flux as a constraint for the ν flux calculation are also very important. The results of several measurements at high altitude with detectors on balloons are in the process of being analysed. New precise measurements of the muon flux at ground level can also be very important.

11. Acknowledgements

I would like to thank Milla Baldo Ceolin for the possibility of participating to this workshop, and Giuseppe Battistoni, Alfredo Ferrari, Tom Gaisser, Maurizio Lusignoli, Todor Stanev, and Yoichiro Suzuki for very useful discussions.

1. Super-Kamiokande coll.(Y. Fukuda *et al.*), Phys.Rev.Lett. 81, 1562 (1998).
2. K.Scholberg this Proceedings also in hep-ex/9905016.
3. Kamiokande collaboration (K.S. Hirata *et al.*), Phys. Lett. B 205, 416 (1988); Phys. Lett. B 280, 146 (1992); (Y. Fukuda *et al.*), Phys. Lett. B 335, 237 (1994).
4. IMB collaboration, (D. Casper *et al.*), Phys. Rev. Lett. 66, 2561 (1991); IMB collaboration, (R. Becker-Szendy *et al.*), Phys.Rev. D 46, 3720 (1992).
5. Soudan 2 Collaboration (W.W.M. Allison *et al.*), Phys.Lett. B 449, 137 (1999); A. Mann, these Proceedings.
6. NACRO collaboration (M. Ambrosio *et al.*), Phys.Lett. B 434, 451 (1998); F. Ronga (for the MACRO collaboration), in Proceedings of Neutrino'98, Takayama, Japan, (1998), hep-ex/9810008.
7. S. Pakvasa these Proceedings.
8. P. Lipari & M. Lusignoli, Phys. Rev. D to appear (1999), and hep-ph/9901350.
9. G. Barr, T.K. Gaisser & T.Stanev, Phys. Rev. D 39 (1989) 3532; V.Agrawal,T.K.Gaisser,P.Lipari&T.Stanev, Phys.Rev.D53,1314 (1996).
10. M. Honda, T. Kajita, K. Kasahara & S. Midorikawa, Phys. Rev. D52 (1995) 4985.
11. E. V. Bugaev and V. A. Naumov, Phys. Lett. B 232, 391, (1989).
12. H. Lee and Y. S. Koh, Nuovo Cimento B 105, 883 (1990).
13. A. Ferrari and P.R. Sala, ATLAS internal note ATL-PHYS-97-113 (accessible at <http://atlasinfo.cern.ch/Atlas/GROUPS/notes.html>) and Proc. of the "Workshop on Nuclear Reaction Data and Nuclear Reactors Physics, Design and Safety", ICTP, Trieste.

14. G. Battistoni *et al.*, Nuclear Phys. B (Proc. Suppl.) 70 (1998) 358.
15. Super-Kamiokande collab. (Futagami *et al.*), hep-ex/9901139, submitted to Phys.Rev.Lett. (1999).
16. Paolo Lipari, T. K. Gaisser & Todor Stanev, Phys. Rev. D 58, 073003 (1998).
17. P. Lipari and M. Lusignoli, Phys. Rev. D 57, 3842 (1998).
18. See the contributions of K.Scholberg, M.Spinetti and S.Mikheyev in these Proceedings.
19. T.K. Gaisser, M. Honda, K. Kasahara, H. Lee, S. Midorikawa, V. Naumov & Todor Stanev, Phys. Rev. D 54, 5578 (1996).
20. T.K.Gaisser, in Proceedings of neutrino 98, Takayama, Japan, hep-ph/9811314; and hep-ph/9811315 (1998).
21. P. Lipari, M. Lusignoli, and F. Sartogo, Phys.Rev.Lett. 74, 4384 (1995).
22. W.R. Webber, R.L. Golden & S.A. Stephens, Proc. 20th ICRC (Moscow) vol. 1 (1987) 325.
23. E.S. Seo, *et al.*, Ap. J. 378 (1991) 763.
24. W. Menn, *et al.*, Proc. 25th ICRC (Durban) vol. 3 (1997) 409.
25. G. Barbiellini, *et al.*, Proc. 25th ICRC (Durban) vol. 3 (1997) 369. Also, M. Boezio *et al.*, (1998) (to be published).
26. S.Orito, *et al.*, talk presented by T. Sanuki at the Symposium "New Era in neutrino Physics", Tokyo Metropolitan University, June 1998.
27. M. Circella, these Proceedings; and hep-ex/9905012, to appear in Phys. Rev.D.
28. J.W. Bieber in Proceedings of the 24th ICRC. Il Nuovo Cimento 19, 777, (1996).
29. The data for a large array of neutron monitors can be obtained in <http://ulysses.uchicago.edu/NeutronMonitor/>.
30. G. Lemaître and M.S. Vallarta, Phys. Rev. 43, 87, (1933).
31. C. Störmer, Astrophysics 1, 237 (1930).
32. D.J.Cooke Phys.Rev.Lett. 51, 320, (1983).
33. P. Lipari & T. Stanev, Proc. 24th ICRC (Rome) vol. 1 (1995) 516.
34. P. Kiraly, in Proceedings of 21st ICRC, vol. 11, 227 (1990).
35. Paolo Lipari, Astroparticle Physics 1, 11, (1992)
36. J.V. Allaby *et al.*, CERN Yellow Report 70-12 (unpublished); T.Eichten *et al.*, Nucl. Phys. B 44, 333 (1972).
37. R.A. Smith and E.J. Moniz, Nucl. Phys. B 43, 605 (1972).
38. J. Engel, E. Kolbe, K. Langanke & P. Vogel, Phys. Rev. D 48, 3048 (1993).
39. J. Marteau, hep-ph/9902210 (1999).
40. D.Rein, L.Sehgal Annals of Physics 133, 79 (1981).
41. R.P.Feynman, M.Kislinger, F.Ravndal Phys.Rev. D 3, 2706 (1971).
42. C.H. Albright and C. Jarlskog, Nucl.Phys. B 84, 467 (1975).
43. M. Gluck, E. Reya and A. Vogt, Z. Phys. C 67, 433 (1995).
44. H.Sobel, these Proceedings.

45. O.C. Allkofer, O.C. Karstensen and W.D. Dau, Phys. Lett. B 425 (1971).
46. B.C. Rastin, J. Phys. G 10, 1629 (1984).
47. M.P. De Pascale *et al.*, J. Geophys. Res. 98, 3501 (1993).
48. J. Kremer for the Caprice collaboration, talk presented at the “First Arctic Workshop on Cosmic Ray Muons”, Sodankyla (Finland) april 1999. Available at <http://www.cern.ch/CosmoLep/>
49. R. Bellotti, *et al.*, Phys. Rev. D 53, 35 (1996).
50. G. Basini *et al.*, Proc. 25th ICRC (Durban) vol. 6 (1997) 381.
51. J.F. Krizmanic *et al.* Proc. 24th ICRC (Rome) vol. 1 (1995) 593.
52. S. Coutu *et al.* (HEAT collaboration), in Proc. Int. conf. on High Energy Physics (Vancouver, 1998).
53. For a preliminary study on possible detectors on airplanes see in <http://zurab-1.fe.infn.it>
54. J. Losecco, hep-ph/9903310 (1999).
55. This argument was suggested to me by Riccardo Barbieri.